

Early warning indicators via latent stochastic dynamical systems

Lingyu Feng ^{a,b,c}, Ting Gao ^{*a,b,c}, Wang Xiao ^{a,b,c} and Jinqiao Duan ^{† c,d,e}

^a*School of Mathematics and Statistics, Huazhong University of Science and Technology, Wuhan, China*

^b*Center for Mathematical Science, Huazhong University of Science and Technology, Wuhan, China*

^c*Steklov-Wuhan Institute for Mathematical Exploration, Huazhong University of Science and Technology, Wuhan, China*

^d*Department of Mathematics and Department of Physics, Great Bay University, Dongguan, China*

^e*Dongguan Key Laboratory for Data Science and Intelligent Medicine, Dongguan, China*

January 2, 2024

Abstract

Detecting early warning indicators for abrupt dynamical transitions in complex systems or high-dimensional observation data is essential in many real-world applications, such as brain diseases, natural disasters, financial crises, and engineering reliability. To this end, we develop a novel approach: the directed anisotropic diffusion map that captures the latent evolutionary dynamics in the low-dimensional manifold. Then three effective warning signals (Onsager-Machlup Indicator, Sample Entropy Indicator, and Transition Probability Indicator) are derived through the latent coordinates and the latent stochastic dynamical systems. To validate our framework, we apply this methodology to authentic electroencephalogram (EEG) data. We find that our early warning indicators are capable of detecting the tipping point during state transition. This framework not only bridges the latent dynamics with real-world data but also shows the potential ability for automatic labeling on complex high-dimensional time series.

Keywords: Directed anisotropic diffusion map; Latent stochastic dynamical system; Transition phenomena; Early warning indicator

Leading Graph: In various practical scenarios, high-dimensional temporal processes are commonly observed. One particularly intriguing challenge involves the analysis of complex patterns in brain activities. The inherent complexity of modeling brain dynamics is exacerbated by the multiple EEG signals. To address this, we have introduced a directed anisotropic diffusion map method, which enables the extraction of latent dynamics in a lower-dimensional manifold. This approach proves valuable in identifying early warning signals for critical changes. Our framework establishes a connection between the latent transition dynamics modeled through stochastic dynamical systems and the real-world high-dimensional EEG data.

1 Introduction

High-dimensional evolutionary processes exist in many real-world systems, such as time-varying patterns of protein folding and unfolding, climate change, and artificial intelligence-assisted disease diagnosis [1–3]. Among these, one fascinating problem is studying complex brain activities over time, which also poses a challenge regarding the limited high-quality labeled data and multi-scale neuron models at different levels. Problems arise from modeling brain dynamics in high-dimensional space due to the complexity of the human brain system. Most of the multi-scale data-driven modeling

*Corresponding author Ting Gao: tgao0716@hust.edu.cn; tinggao0716@gmail.com

†Jinqiao Duan: duan@gbu.edu.cn; duanjq@gmail.com

approaches build surrogate models for brain activities. Electroencephalogram (EEG) signals are collected by dozens of electrodes placed on the scalp. Considering the low-dimensional representation from observations in electrophysiological experiments, neuroscientists have been investigating the latent dynamics of the brain via various dimension reduction techniques. Moreover, it shows that dimension reduction techniques lead to significantly enhanced performance by removing multi-collinearity and avoiding the curse of dimensionality.

One methodology for learning low-dimensional latent dynamics comes from the variational auto-encoder framework, which ability to simultaneously reduce dimensionality while learning latent dynamics [4]. However, the disadvantages include the high computational cost, inaccuracy of reconstructed data, as well as weak explanation of effective coordinates of reduced systems. Therefore, other manifold learning methods are highly investigated to represent the dataset on a low-dimensional embedding space. Multiple studies consistently demonstrate that nonlinear manifold learning algorithms outperform linear ones. Among several effective nonlinear manifold learning methods, diffusion maps are widely used to analyze dynamical systems [5] and stochastic dynamical systems [6] on low-dimensional latent space, determine order parameters for chain dynamics [7], classify person from electrocardiogram recordings [8], and so on. Also, dynamics of brain activity from task-dependent functional magnetic resonance imaging data are modeled by a three-step framework including diffusion maps in [9]. Besides, the double diffusion maps on the latent space allow the approximation of the reduced dynamical models [10]. Further, the directed anisotropic diffusion map improves upon the isotropic diffusion by incorporating the local information. It considers the original data structure and adapts the diffusion process accordingly. Inspired by this and to efficiently distinguish between epilepsy-related data and pre-ictal data in the latent space, we add a drift function in the directed diffusion to construct an anisotropic diffusion map.

After dimension reduction through manifold learning, the latent dynamics could be learned in either deterministic or stochastic ways. For example, Talmon et al. study the inference of latent intrinsic variables of dynamical systems from observed output signals [11]. Also, for partially observed data, Ouala et al. introduce a framework based on the data-driven identification of an augmented state-space model using a neural-network-based representation [12]. On the other hand, since stochastic differential equations are usually used to model nonlinear systems that involve uncertainty or randomness [13], it is of great interest to learn latent stochastic differential equations from real high dimensional data. To gain deeper insights into the latent characteristics, researchers frequently investigate the stochastic dynamical systems, which depend on the geometry and distribution of the latent space. For instance, Evangelou et al. combine diffusion map and Kramers–Moyal to construct a reduced, data-driven, parameter-dependent effective stochastic differential equation for electric-field mediated colloidal crystallization [14]. Besides, in general cases when the noise is non-Gaussian Lévy motion, there are various methods to realize the stochastic dynamical systems evolving in the latent space over time [15], as well as the corresponding transition dynamics [16,17].

In real world applications for complex disease diagnosis, early warning detection has attracted a great deal of attention for a long time. For instance, epilepsy is a neurological disease characterized by recurrent and unpredictable seizures, which are sudden bursts of abnormal brain activity. According to the World Health Organization, epilepsy affects around 50 million people worldwide, making it one of the most prevalent neural diseases. However, the mechanisms governing seizure activity are not well understood and many patients suffer a lot. Early detection and intervention of epileptic seizures can help patients receive timely and appropriate treatment, which might prevent or minimize the negative impacts of seizures on their health and quality of life. Liu et al. present a model-free computational method to detect critical transitions with strong noise by dynamical network markers [18]. Bury et al. develop a deep learning algorithm that provides early warning signals in systems by exploiting information of dynamics near tipping points [19]. In reality, the diagnosis of epilepsy requires experienced medical professionals. Diagnosis of epilepsy requires an experienced medical professional. Analyzing extensive EEG data to determine the onset of an epileptic seizure is a time-consuming and labor-intensive process. Additionally, relying on visual recognition can result in doctors inaccurately assessing the timing of the epilepsy occurrence. Therefore, in this paper, we propose to automatically detect the early warning signals from the latent stochastic dynamical system by introducing the Onsager-Machlup indicator, sample entropy, and transition probability.

In summary, the goal of the present study is to model and analyze the brain activity data from epileptic patients to identify early warnings of epileptic seizures, with stochastic dynamical systems

tools. Our main contributions are

- Find the appropriate low-dimensional coordinates from time evolutionary high-dimensional data;
- Learn the latent stochastic differential equation and dynamics on low-dimensional manifold;
- Explore effective early warning indicators for transitions in brain activity.

The remainder of this paper is structured as follows. In Section 2, we first design a drift function to obtain better low dimensional representation by the directed anisotropic diffusion map. Following that, we extract the latent stochastic dynamical system from high dimensional dataset, and establish specific early warning indicators. In Section 3, we validate our framework by numerical experiments on real EEG data. Finally, we summarize our results together with some conclusions in Section 4.

2 Methodology

In this section, we introduce the main procedures in our workflow of exploring early warning signals from latent dynamical systems (Fig. 1).

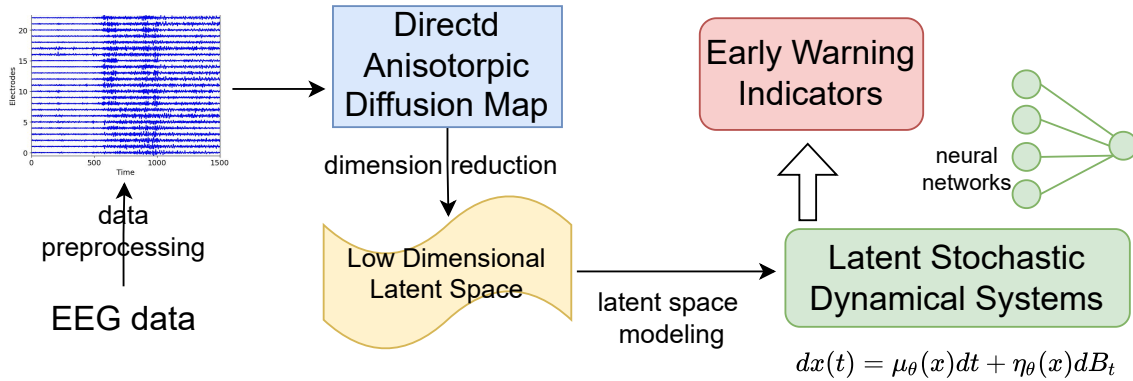


Figure 1: A schematic diagram of our framework.

2.1 Anisotropic Diffusion Map

The core idea of diffusion map is a time-dependent diffusion process, i.e., a random walk on the dataset where each hop has the associated transition probability. When the diffusion process runs, for each step, we can calculate the distance over the underlying geometric structure. To evaluate the connectivity strength between two data points or the probability of jumping from x to y in one step of the random walk, we need to introduce a diffusion kernel.

Let X be the dataset in \mathbf{R}^n . Define a kernel k on X satisfying:

- k is symmetric, i.e. $k(x, y) = k(y, x)$,
- k is positivity preserving, i.e. $k(x, y) \geq 0$.

This kernel captures how closely the points in X related to each other. It characterizes the connection between pairs of points within the symmetric graph, where the weight is determined by the kernel function k . The transition probabilities defined by the weight function in the graph directly reflect the local geometry. The technique to obtain the latent diffusion space is known as the normalized graph Laplacian construction [20]. Let \mathcal{M} be a compact smooth manifold and $\mathcal{M} = \Phi(\mathcal{M})$, $\Phi : \mathcal{M} \rightarrow \mathbf{R}^d$ denote an isometric embedding into d -dimensional Euclidean space. Assume that the dataset X is the entire manifold and $q(x)$ represents the density of the points on \mathcal{M} .

The isotropic diffusion computes all directions equally. It means that all variables in dataset play the same role. However, some variables might be more important than others under the prior knowledge

of the dataset. The anisotropic diffusion is sometimes more useful to locally separate the variables and provides early warnings.

The function ∇f defined on dataset can be obtained through derivation. To design a diffusion process adapted to the dataset, consider the directed kernel

$$k_\varepsilon(x, y) = \exp\left(-\frac{\|x - y\|^2}{\varepsilon} - \frac{\|\nabla f(x) \cdot x - \nabla f(y) \cdot y\|^2}{\varepsilon^2}\right), \quad (1)$$

where $x, y \in \mathbf{R}^n$ and $\|\cdot\|$ denotes the Euclidean norm. The directed kernel will promote the formation of connections among points within some close distances while also creating greater separation for distant points.

We adopt directed diffusion to show that the construction of diffusion kernel can be data-driven. The weight matrix K corresponds to an anisotropic kernel on the observable space X , where the anisotropy is measured by the gradient f . By integrating over the second variable k_ε , the density d_ε is represented by

$$d_\varepsilon(x) = \int_X k_\varepsilon(x, y) q(y) dy,$$

and define

$$p_\varepsilon(x, y) = \frac{k_\varepsilon(x, y)}{d_\varepsilon(x)}. \quad (2)$$

The directed operator P_ε is defined by

$$P_\varepsilon f(x) = \int_X p_\varepsilon(x, y) f(y) q(y) dy. \quad (3)$$

Dealing with finite data points, we should approximate integrals by finite sums and can describe the latent reduced order space by the spectral analysis. For most applications, we consider the bounded part will consist of a finite number of points. Here, the eigenvalues of the directed diffusion operator are distributed between 0 and 1. In other words, we have $1 = \lambda_0 \geq \lambda_1 \geq \lambda_2 \geq \dots$ with $\lambda_i \geq 0$. Since the first eigenvalue $\lambda_0 = 1$ and the eigenvector is a constant vector, the first d eigenvalues starting from λ_1 and the corresponding eigenvectors capture the main features. The directed anisotropic diffusion map is given by $\Phi(x) = [\lambda_1 \phi_1(x) \dots \lambda_d \phi_d(x)]^T$, where $\{\phi_i\}_{i=1}^d$ are eigenvectors. Several benefits are obtained by dimension reduction. It is well known that high dimensionality often degrades the dynamical performance, necessitating the use of lower-dimensional representations. Additionally, in the latent space, there is a significant reduction in the time required to train a model.

2.2 Extracting the Latent Stochastic Dynamical System

In order to depict the broader spectrum of nonlinear dynamics in the latent space, we proceed to the construction of the reduced order models. Here, the stochastic differential equations are preferred to carry the latent dynamics of the high-dimensional data. The drift term (vector field) characterizes the deterministic aspect of the system. While the diffusion term (fluctuation) pertains to the stochastic component of the system and depends on a random process, such as Brownian motion or Lévy process.

Let $z(t)$ be a stochastic variable governed by the stochastic differential equation

$$dz(t) = \mu(z(t))dt + \eta(z(t))dB_t, \quad (4)$$

where $\mu : \mathbf{R}^d \rightarrow \mathbf{R}^d$ is the drift term, $\eta : \mathbf{R}^d \rightarrow \mathbf{R}^{d \times d}$ is the diagonal diffusivity matrix, and B_t is \mathbf{R}^d independent Brownian motion. Inspired by deep learning architecture [21], we construct two neural networks μ_θ and η_θ to estimate μ and η , whose inputs and weights are represented by the basis functions and coefficients, respectively.

In fact, we have access to a set of lower-dimensional points $\{z(t_i)\} \in \mathbf{R}^d$ by directed anisotropic diffusion map. Then the set of snapshots $\{z(t_{i+1}), z(t_i), \delta_t\}$, $\delta_t = t_{i+1} - t_i$ is available. Over the small time interval $[t_i, t_{i+1}]$, the stochastic differential equation has a discrete form

$$z(t_{i+1}) = z(t_i) + \mu(z(t_i))\delta_t + \eta(z(t_i))\delta B_t,$$

where $\delta B_t^j = B_{t_{i+1}}^j - B_{t_i}^j \sim \mathcal{N}(0, \delta_t)$, $j = 1, \dots, d$. Conditioned on $(z(t_i), \delta_t)$, the point $z(t_{i+1})$ obeys a multivariate normal distribution

$$z(t_{i+1}) \sim \mathcal{N}(z(t_i) + \delta_t \mu(z(t_i)), \delta_t \eta(z(t_i))^2).$$

Hence, the neural networks are trained by minimizing the loss function $\mathcal{L}(\theta)$, which is defined as

$$\mathcal{L}(\theta) = \frac{(z(t_{i+1}) - z(t_i) - \delta_t \mu_\theta(z(t_i)))^2}{\delta_t \eta_\theta(z(t_i))^2} + \log |\delta_t \eta_\theta(z(t_i))^2| + \log(2\pi). \quad (5)$$

Moreover, depending on the tail property of the real dataset, the latent space modelling can be extended to stochastic differential equations driven by non-Gaussian noise [22].

2.3 Early Warning Indicators

When existing latent variables in complex disease processes, a critical concern revolves around the concept of early warning indicators. To identify abrupt changes and issue early warnings, we introduce the indicators by Onsager-Machlup action functional, sample entropy, and transition probability.

2.3.1 Onsager-Machlup Indicator

Consider the following stochastic differential equation in the state space \mathbb{R}^m

$$dz_t = \mu(z_t)dt + \eta dB_t, \quad t > 0,$$

where $\mu : \mathbb{R}^m \rightarrow \mathbb{R}^m$, B_t is a standard m -dimensional Brownian motion, and η is a diagonal matrix with positive constants. Onsager and Machlup are the first to consider the probability of paths of a diffusion process as the starting point of a theory of fluctuations [23]. The outcome of a functional integral over the process paths is subsequently termed the Onsager-Machlup function, denoted by

$$S_X^{OM}(\psi) = \frac{1}{2} \int_0^T \left[\frac{|\dot{\psi}(s) - \mu(\psi(s))|^2}{\eta^2} + \nabla \cdot \mu(\psi(s)) \right] ds,$$

where ψ is a curve in \mathbb{R}^m .

Let time series $z(t)$ be a stochastic variable governed by the stochastic differential equation in the latent space. Recalling Sec. 2.2, two neural networks μ_θ and η_θ are constructed to estimate μ and η , whose inputs and weights are represented by the basis functions and coefficients, respectively. Here, we define the Onsager-Machlup indicator by

$$OM(l, t) = \frac{1}{2} \int_{t-l+1}^t \left[\frac{|\dot{z}(s) - \mu_\theta(z(s))|^2}{\eta_\theta^2} + \nabla \cdot \mu_\theta(z(s)) \right] ds, \quad (6)$$

where \dot{z} is the derivative function written as

$$\dot{z}(s) = \frac{z(s+ds) - z(s-ds)}{2ds}.$$

If there are notable variations in Onsager-Machlup indicator, we will issue an early warning.

2.3.2 Sample Entropy Indicator

Sample entropy, introduced by Richman and Moorman [24], serves as a statistical metric for quantifying the complexity of time series data. It is particularly effective in capturing self-similarity and irregularity, making it a robust tool for analyzing complex systems. For d interdependent time series, we introduce the multidimensional sample entropy to measure the latent system complexity [25]. Specifically, it approximately equals to the negative natural logarithm of the conditional probability that two sub-sequences similar for consecutive data points remain similar for the next p time points, where the sub-sequences can originate from either the same or different time series.

For d time series $z^\alpha(t)$ ($\alpha = 1, \dots, d$), the sequence of l time to compute the sample entropy is expressed by $Z(t_l) = \{z^\alpha[t_1 : t_l], \alpha = 1, \dots, d\}$, where $z^\alpha[t_1 : t_l] = \{z^\alpha(t_1), \dots, z^\alpha(t_l)\}$. There forms the vectors $Z_k^\alpha(m, q) = \{z^\alpha[kq + 1 : kq + m]\} \subset Z(t_l)$ ($k = 1, 2, \dots$). The distance between two vectors is defined to be the Chebyshev distance

$$d(Z_i^\alpha(m, q), Z_j^\beta(m, q)) = \max\{|x^\alpha(iq + s) - x^\beta(jq + s)|, 1 \leq s \leq m\}.$$

If the superscripts $\alpha = \beta$, the subscripts $i \neq j$. Assume that two vectors are close if their distance $d(Z_i^\alpha(m, q), Z_j^\beta(m, q)) < r \max\{\sigma^\alpha, \sigma^\beta\}$, where r is the tolerance for accepting matches and σ^α and σ^β are the standard deviations, allowing measurements on dataset with different amplitudes to be compared. Now we consider a set $A(m + p, q)$ of all vectors satisfying $Z_k^\alpha(m + p, q) \subset z^\alpha[t_1 : t_l]$ and $\alpha = 1, \dots, d$. Note that the maximum of k in $A(m + p, q)$ is n_z . To make the number of vectors of length m equal to that of length $m + p$, the set $B(m, q)$ is characterized as $\{Z_k^\alpha(m, q) : Z_k^\alpha(m, q) \subset z^\alpha[t_1 : t_l], 1 \leq \alpha \leq d, 1 \leq k \leq n_z\}$. Define $B(m, q, r, l)$ as the number of close vectors in $B(m, q)$. Similarly, denote the number of close vectors in $A(m + p, q)$ by $A(m + p, q, r, l)$. Hence, the sample entropy for multidimensional system is represented by

$$SampEn(m, p, q, r, l) = -\log \left(\frac{A(m + p, q, r, l)}{B(m, q, r, l)} \right),$$

in the time interval $[t_1, t_l]$. The parameters l, m, p, q and r must be fixed for each calculation. There is no confusion about the parameters, so in time window $[t - l + 1, t]$

$$SampEn(t) = -\log \left(\frac{A(m + p, q, r, l)}{B(m, q, r, l)} \right). \quad (7)$$

In the event of significant fluctuations in sample entropy, we will give an early warning.

2.3.3 Transition Probability Indicator

The transition probability between two states is defined in [26]. The phase space for the latent variable is separated into two regions A and B and the ratio TP_{AB} is defined as

$$TP_{AB}(t) = \frac{\langle I_A(z(0))I_B(z(t)) \rangle}{\langle I_A(z(0)) \rangle}, \quad (8)$$

where I_A is an indicator function satisfying $I_A(z) = 1$ if $z \in A$, and $I_A(z) = 0$ if $z \notin A$ and $\langle \cdot \rangle$ denotes the ensemble average. The ratio TP_{AB} represents the probability of finding the system in region B after time t under the condition $z(0) \in A$. In the following, if the probability is more than 0.5, we will give an early warning due to higher transition probability.

3 Experiments

We now apply the method outlined in the previous sections to datasets collected from patients with epileptic seizures. Our objective is to analyze the latent dynamics and illustrate our early warning strategy.

3.1 Data Preprocessing

Electroencephalogram (EEG) entails the capture of signals using electrodes positioned on the scalp, thereby recording the electrical activity during epileptic seizures. The EEG dataset encompasses both pre-ictal and ictal data, organized in a matrix format of channels over time, with a sampling rate of 256 points per second. To facilitate analysis, each electrode signal undergoes rescaling to an interval of $[-0.5, 0.5]$ and is subsequently subsampled by averaging every sixteen points, resulting in the formation of the dataset. In Fig. 2, there is a sample image that the doctor labels $Time = 500$ as the separation time for pre-ictal and ictal period. As different doctors may assign varying labels over time, here $Time = 500$ is utilized as a reference.

3.2 Dimension Reduction with Directed Anisotropic Diffusion Map

To construct the diffusion matrix, the data from all electrodes at each time point is viewed as a high-dimensional node in the diffusive graph. Notably, electrode signals display abnormal fluctuations preceding the onset of an epileptic seizure. Timely detection of abnormalities in electrical signals holds the potential to provide early warnings for epileptic seizures. Such early warnings can enable specific intervention measures aimed at mitigating or avoiding epileptic seizures. We suggest identifying early warnings within a lower-dimensional space through the application of directed anisotropic diffusion maps.

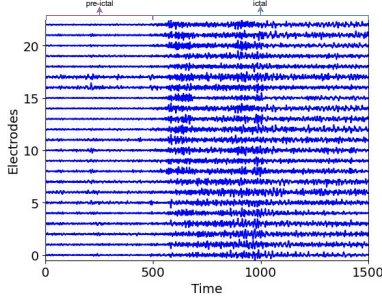


Figure 2: An example: the EEG data of a patient.

3.2.1 Diffusion Matrix and Spectral Gap

The diffusion matrix is constructed by the diffusion kernel and shows the transition among all high-dimensional nodes in the diffusive graph, which exhibits the transition probability from one point to another. The directed drift term $\nabla f(x) = |\dot{x}|$ is data-driven, where

$$\dot{x} = \frac{1}{2} \left(\frac{x(t_{i+1}) - x(t_i)}{t_{i+1} - t_i} + \frac{x(t_i) - x(t_{i-1})}{t_i - t_{i-1}} \right).$$

Then we apply the directed diffusion to the preprocessed dataset. The drift term can be thought as an enhanced force.

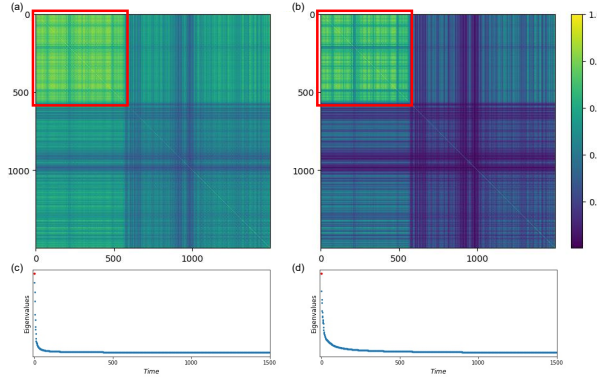


Figure 3: Comparison of diffusion map and directed anisotropic diffusion map. The top row presents the kernel matrices, and the bottom row represents the eigenvalues. For all cases, the plots we show here are under $\epsilon = 1$: left column ((a)(c)) is constructed when $\nabla f = 0$, while the right column ((b)(d)) is calculated when $\nabla f(x) = |\dot{x}|$.

As shown in the top row of Fig. 3, most points have a measure greater than 0.5 with another point in (a), indicating that the transition probability to other points is equivalent. In (b), the data points within the red frame have higher transition probabilities to each other, while the transition probabilities to the points outside gradually decrease. Through directed diffusion, the transition probability of sample points inside the red box to outside the red box is reduced. Correspondingly, the transition probability from the sample point outside the red box to the data point inside the red box also decreases accordingly. In this way, the diffusion activity intensity between the points inside the red box and the points outside the red box in the original high-dimensional time series is forced to attenuate, so the two regions will be better separated.

The diffusion matrix has a discrete sequence of eigenvalues $\{\lambda_i\}_{i \geq 1}$ and eigenvectors $\{\phi_i\}_{i \geq 1}$ such that $1 \geq \lambda_1 \geq \lambda_2 \geq \dots$. The eigenvalues affect diffusive strength, and the spectral gap is an indicator to help us find the effective dimension of latent space. In the bottom row of Fig. 3, the first five eigenvalues of the diffusion map have similar gaps, while the first eigenvalue of the directed anisotropic diffusion map shows a distinct spectral gap from the second one. Then the largest eigenvalue is separated from the others.

3.2.2 Low-dimensional Embedding over Time

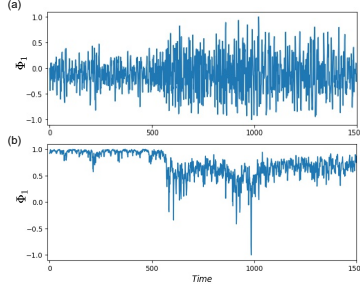


Figure 4: Comparison of low-dimensional embedding patterns with (a) diffusion map ($\nabla f = 0$) and (b) directed anisotropic diffusion map ($\nabla f = |\dot{x}|$).

The directed anisotropic diffusion map discovers a latent coordinate denoted as Φ_1 by the gap between two adjacent eigenvalues, as shown in Fig. 3 bottom row. This suggests that the first diffusion coordinate is enough to provide an economical representation of the original EEG dataset. We check the interpretability of the data-driven observations by displaying the coordinates in Fig. 4. The diffusion map projects data points to divergent locations. Moreover, the anisotropic diffusion map partitions the dataset into two states with a distribution shift in the latent space, expended by the first leading diffusion coordinate. From (a) in Fig. 4, the data points are fluctuant all the time with the same expectation. However, in (b), the drift term induced by the gradient of data $\nabla f(x)$ helps to differentiate two groups of points at $Time \approx 600$ with different expectations.

3.3 Latent Stochastic Dynamical Systems

An interesting aspect of our research involves the dynamic behaviors exhibited by latent dynamical systems. In this section, we aim to elucidate the connection between the latent stochastic differential equation and the original high-dimensional time evolutionary data.

Following dimension reduction through the directed anisotropic diffusion map, we obtain the projected dataset onto the first diffusion coordinate Φ_1 . The projected data plotted over time displays the transition between two states: pre-ictal state and ictal state. Therefore, we assume that the stochastic differential equation in the latent space has two meta-stable states and rescale the data to an interval of $[-1, 1]$ for convenience. Given data in Fig. 4 (b), we would like to obtain the latent stochastic differential equation in the form of Eq. (4). To get meaningful representations of drift and diffusion coefficients, we assume the utilization of a polynomial basis for approximating both $\mu(z)$ and $\sigma(z)$ and employ neural networks to approximate the latent equations. The inputs of networks are the basis functions of the coordinates and the time step is 0.0625. The latent space contains 1500 time points and 1499 pairs of $\{(z(t_{i+1}), z(t_i))\}$ are available. We randomly select 1200 pairs to train the networks and validate the identification accuracy on the rest 299 pairs.

To find the explicit form of drift and diffusion coefficients in the unknown stochastic differential equations, all the unknown drift and diffusion terms are parameterized with neural networks, with a polynomial basis as the input vector. Then using the loglikelihood method in Sec. 2.2, the learnt stochastic differential equation under the coordinate Φ_1 has the form

$$dz(t) = \mu_1(z(t))dt + \sigma_1(z(t))dB_t, \quad (9)$$

where $\mu_1(z) = 0.0219 + 0.7128z - 0.0774z^2 - 1.1677z^3$, and $\eta_1(z) = -0.5115$.

Moreover, we adopt density as the validation metric for the testing data (consisting of 299 pairs). In Fig. 5, we compare the density of the estimated $z(t_{i+1})$ obtained through the approximation of the latent stochastic differential equation (Eq. (9)) with that of the ground truth from corresponding data points in Fig.4(b). The alignment between our approximation and the true data density is evident. Additionally, the presence of two peaks in the density plot signifies the existence of two meta-stable states.

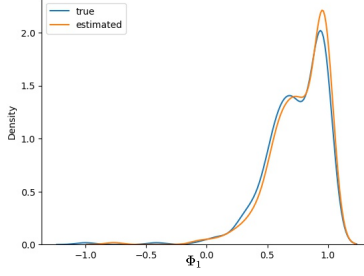


Figure 5: The validation of the neural network approximation with regard to Φ_1 .

3.4 Early Warning Indicators

In this section, we present the time varying indicators resulted from transitions in the latent space.

Onsager-Machlup Indicator and Sample Entropy Indicator

For Φ_1 , we employ a time series trace comprising 1500 data points to calculate the indicator over time and compare it with the standard deviation. The time window l is set to 100, moving forward in each time unit. The Onsager-Machlup indicator is computed in each time window using the Eq. (6). When applying the Eq. (7) to compute the sample entropy, the parameters are kept constant at $m = 10$, $p = 1$, $q = 4$, and $r = 0.5$. The values of the two indicators over time are depicted in red in Figure 6 and the standard deviation is in green.

Assume that a transition will occur if the indicator surpasses a predefined threshold. Two patterns are observed in the coordinate signal over time. Until approximately 600, the Onsager-Machlup indicator remains negative, and the sample entropy consistently equals 0. In contrast, the standard deviation, commonly employed as an indicator, undergoes a change at $Time \approx 200$. This could lead to erroneous judgments. This implies that both the Onsager-Machlup indicator and the sample entropy indicator offer more precise warning points compared to the standard deviation. Consequently, this identified change point can assist doctors in distinguishing between pre-ictal and ictal periods, facilitating automated labeling processes.

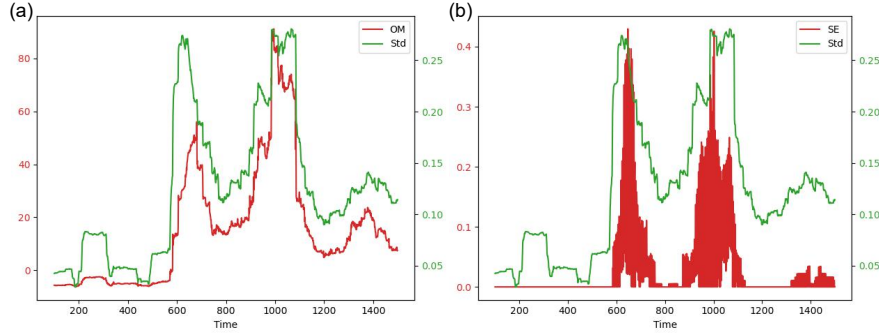


Figure 6: The Onsager-Machlup indicator (a) and the sample entropy (b) of raw data projected onto coordinate Φ_1 , compared with the standard deviation (green).

Transition Probability Indicator

Assigning the width of each time window as 100, Fig.7 shows the transition probability. The first 100 points are selected as starting points, generating 100 samples. The split point is set as 0.8, delineating regions $A = [0.8, \infty)$ and $B = (-\infty, 0.8)$. In Fig. 7, we calculate the transition probability by Eq. (8) of state for each time step t starting from the initial state. Assuming a transition occurs when the probability surpasses 0.5, we designate the point with a probability equal to 0.5 as the warning point. Over time, distinct patterns emerge in the signal of the first coordinate, with warning point occurring around $Time = 600$ for Φ_1 .

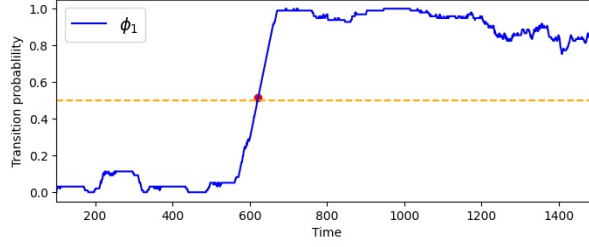


Figure 7: The transition probability of raw data projected onto coordinate Φ_1 . The red dot indicates the transition probability equal to 0.5.

4 Conclusion

Predicting epileptic seizures from brain signals is inherently challenging and time-consuming, primarily due to the high dimensionality and complexity of the data. In this paper, we propose an efficient method for automatically identifying abnormalities in EEG signals. Our approach leverages directed anisotropic diffusion map for dimensionality reduction and establishes a stochastic dynamical system model in the low-dimensional latent space. This enables effective and time-saving detection of early warning signals associated with epilepsy.

Directed diffusion is employed to differentiate ictal data from pre-ictal data under the notion that information can flow in a specific direction. This technique serves as an extension of the diffusion map algorithm, specifically tailored to extract and represent the underlying structure and relationships in high-dimensional data. A crucial factor in defining a reduced latent space is the presence of a spectral gap among the eigenvalues. In this paper, we focus on effective coordinates that capture the dynamic characteristics of the original high-dimensional data.

Early warning of epileptic seizures is of paramount importance for individuals with epilepsy. The abrupt change is caught for early warning in the latent space, where normal state and ictal state can be viewed as two meta-stable states. The ability to identify transitions between meta-stable states plays a pivotal role in predicting and controlling brain behavior. We employ stochastic differential equations to model the nonlinear dynamics in the latent space. Furthermore, we derive three effective warning signals—namely, the Onsager-Machlup Indicator, Sample Entropy Indicator, and Transition Probability Indicator—utilizing information from the latent coordinates and the latent stochastic dynamical systems. These indicators enhance the robustness and accuracy of early warning systems for epileptic seizures. This framework of learning latent stochastic systems and detecting abnormal dynamics has the potential to extend to general scenarios for other complex high dimensional time evolutionary data.

Acknowledgements

We would like to thank Professor Quanying Liu and her students Yinuo Zhang, Zhichao Liang for providing the data and helpful discussion. This work was supported by the National Key Research and Development Program of China (No. 2021ZD0201300), the National Natural Science Foundation of China (No. 12141107), the Fundamental Research Funds for the Central Universities (5003011053), the Fundamental Research Funds for the Central Universities, HUST: 2022JYCXJJ058 and Dongguan Key Laboratory for Data Science and Intelligent Medicine.

Data availability

The data that support the findings of this study are openly available in GitHub at <https://github.com/LY-Feng/EW-in-latent-SD>.

References

- [1] A. Mardt, L. Pasquali, H. Wu, and F. Noé. Vampnets for deep learning of molecular kinetics. *Nat. Commun.*, 9(1):5, 2018.
- [2] F. Yang, Y. Zheng, J. Duan, L. Fu, and S. Wiggins. The tipping times in an arctic sea ice system under influence of extreme events. *Chaos*, 30(6):063125, 2020.
- [3] P. AM Mediano, F. E Rosas, J. C. Farah, M. Shanahan, D. Bor, and A. B. Barrett. Integrated information as a common signature of dynamical and information-processing complexity. *Chaos*, 32(1), 2022.
- [4] L. Feng, T. Gao, M. Dai, and J. Duan. Learning effective dynamics from data-driven stochastic systems. *Chaos*, 33(4), 2023.
- [5] B. Nadler, S. Lafon, R. R. Coifman, and I. G. Kevrekidis. Diffusion maps, spectral clustering and reaction coordinates of dynamical systems. *Appl. Comput. Harmon. Anal.*, 21(1):113–127, 2006.
- [6] R. R. Coifman, I. G. Kevrekidis, S. Lafon, M. Maggioni, and B. Nadler. Diffusion maps, reduction coordinates, and low dimensional representation of stochastic systems. *Multiscale Model. Simul.*, 7(2):842–864, 2008.
- [7] A. L. Ferguson, A. Z. Panagiotopoulos, P. G. Debenedetti, and I. G. Kevrekidis. Systematic determination of order parameters for chain dynamics using diffusion maps. *PNAS*, 107(31):13597–13602, 2010.
- [8] J. Sulam, Y. Romano, and R. Talmon. Dynamical system classification with diffusion embedding for ecg-based person identification. *Signal Process.*, 130:403–411, 2017.
- [9] I. K. Gallos, D. Lehmberg, F. Dietrich, and C. Siettos. Data-driven modelling of brain activity using neural networks, diffusion maps, and the koopman operator. *arXiv preprint arXiv:2304.11925*, 2023.
- [10] N. Evangelou, F. Dietrich, E. Chiavazzo, and D. et al. Lehmberg. Double diffusion maps and their latent harmonics for scientific computations in latent space. *J. Comput. Phys.*, 485:112072, 2023.
- [11] R. Talmon, S. Mallat, H. Zaveri, and R. R. Coifman. Manifold learning for latent variable inference in dynamical systems. *IEEE Trans. Signal Processing*, 63(15):3843–3856, 2015.
- [12] S. Ouala, D. Nguyen, L. Drumetz, and B. et al. Chapron. Learning latent dynamics for partially observed chaotic systems. *Chaos*, 30(10):103121, 2020.
- [13] J. Duan. *An Introduction to Stochastic Dynamics*, volume 51. Cambridge, 2015.
- [14] N. Evangelou, F. Dietrich, J. M. Bello-Rivas, and A. J. et al. Yeh. Learning effective sdes from brownian dynamic simulations of colloidal particles. *Mol. Syst. Des. Eng.*, 8:887–901, 2023.
- [15] Y. Li and J. Duan. Extracting governing laws from sample path data of non-gaussian stochastic dynamical systems. *J. Stat. Phys.*, 186:1–21, 2021.
- [16] M. Dai, T. Gao, Y. Lu, Y. Zheng, and J. Duan. Detecting the maximum likelihood transition path from data of stochastic dynamical systems. *Chaos*, 30(11):113124, 2020.
- [17] T. Gao, J. Duan, and X. Kan. Dynamical inference for transitions in stochastic systems with α -stable lévy noise. *J. Phys. A Math. Theor.*, 49, 2015.
- [18] R. Liu, P. Chen, K. Aihara, and L. Chen. Identifying early-warning signals of critical transitions with strong noise by dynamical network markers. *Sci. Rep.*, 5(1):17501, 2015.
- [19] T. M. Bury, R. Sujith, I. Pavithran, and M. et al. Scheffer. Deep learning for early warning signals of tipping points. *PNAS*, 118(39):e2106140118, 2021.
- [20] F. Chung. *Spectral graph theory*, volume 92. Am. Math. Soc., 1997.

- [21] F. Dietrich, A. Makeev, G. Kevrekidis, and N. et al. Evangelou. Learning effective stochastic differential equations from microscopic simulations: Linking stochastic numerics to deep learning. *Chaos*, 33(2), 2023.
- [22] C. Fang, Y. Lu, T. Gao, and J. Duan. An end-to-end deep learning approach for extracting stochastic dynamical systems with α -stable lévy noise. *Chaos*, 32(6), 2022.
- [23] L. Onsager and S. Machlup. Fluctuations and irreversible processes. *Phys. Rev.*, 91(6):1505, 1953.
- [24] J. S. Richman and J. R. Moorman. Physiological time-series analysis using approximate entropy and sample entropy. *Am. J. Physiol. Heart Circ. Physiol.*, 278(6):H2039–H2049, 2000.
- [25] J. Meng, J. Fan, J. Ludescher, A. Agarwal, X. Chen, A. Bunde, J. Kurths, and H. J. Schellnhuber. Complexity-based approach for el niño magnitude forecasting before the spring predictability barrier. *PNAS*, 117(1):177–183, 2020.
- [26] Peter G. B., David W. C., Christoph D., and Phillip L. G. Transition path sampling: throwing ropes over rough mountain passes, in the dark. *Annu. Rev. Phys. Chem.*, 53:291–318, 2002.